# Controlled synthesis and upconversion luminescence properties of heterogeneous isomorphism Yb^{3+}/Er^{3+} co-doped $Na_{0.9}Ca_{0.9}Gd_{1.1}F_6$ nanorods with multiple luminescence centers.

Electronic Supplementary Information (ESI)

Ruijun Tang[a], Jianxun Wang[a], Yueshan Xu[a], Shasha Wang*[,a] and Gejihu De*[,a,b]

[a.] College of Chemistry and Environment Science, Inner Mongolia Normal University, Hohhot 010022, China. E-mail: degjh@imnu.edu.cn.

[b.] Key Laboratory of Physics and Chemistry of Functional Materials, Inner Mongolia, Hohhot 010022, China.

1
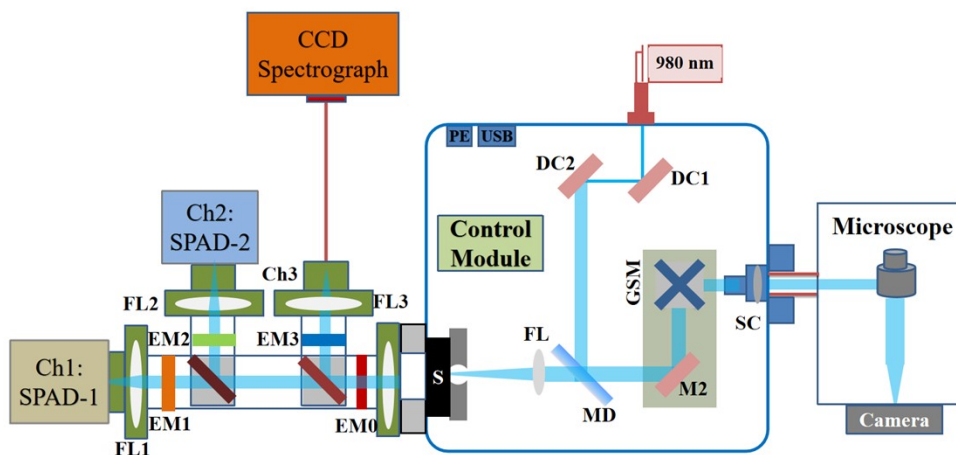
Scheme S1. Confocal microscope imaging system.

Scheme S1 shows the schematic diagram of the imaging system completed on the ISS Q2 confocal laser scanning nanomicroscope. The process has been reported by our group.[1]
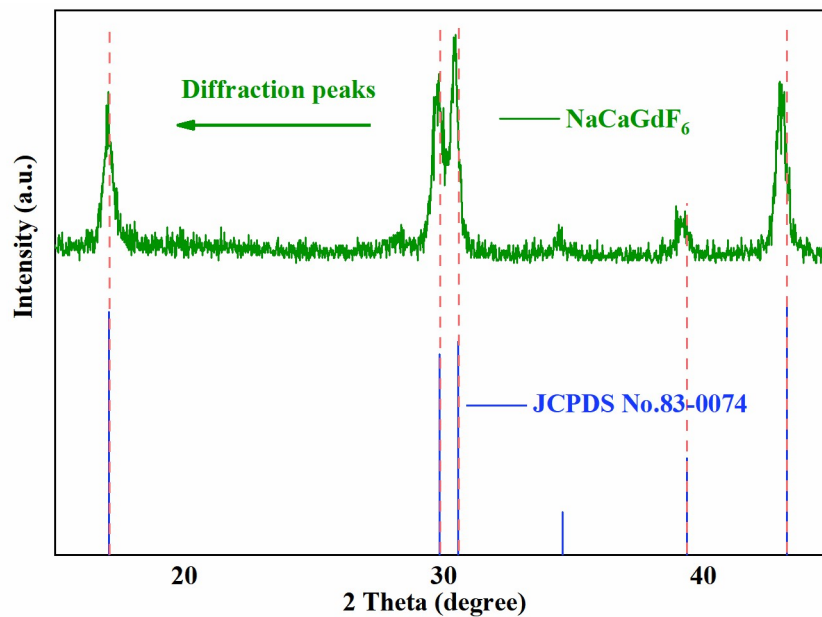

Figure S1. XRD pattern of $Na_{0.9}Ca_{0.9}Gd_{1.1}F_6$:$Yb^{3+}$/$Er^{3+}$ nanorods synthesized at 20 mL OA, 10 mL OC, 5 mL EG, 8 mmol NaF, 200 °C for 48 h.

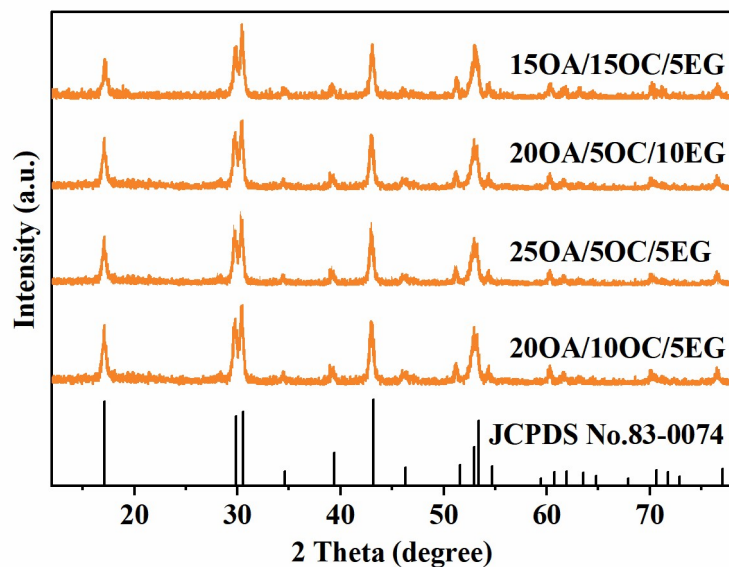**Figure S2.** XRD patterns of $Na_{0.9}Ca_{0.9}Gd_{1.1}F_6$:$Yb^{3+}$/$Er^{3+}$ nanocrystals prepared under different solvent ratios. Other conditions: 8 mmol NaF, 200 °C for 48 h.

Table S1. The average size of $Na_{0.9}Ca_{0.9}Gd_{1.1}F_6$:$Yb^{3+}$/$Er^{3+}$ nanocrystals prepared under different Solvent ratios was calculated using the Debye-Scherrer equation. Other conditions: 8 mmol NaF, 200 °C for 48 h.

Solvent ratio (mL)	sizes (nm)
15mLOA/15mLOC/5mLEG	18.4
20mLOA/5mLOC/10mLEG	22.5
25mLOA/5mLOC/5mLEG	20.1
20mLOA/10mLOC/5mLEG	20.9
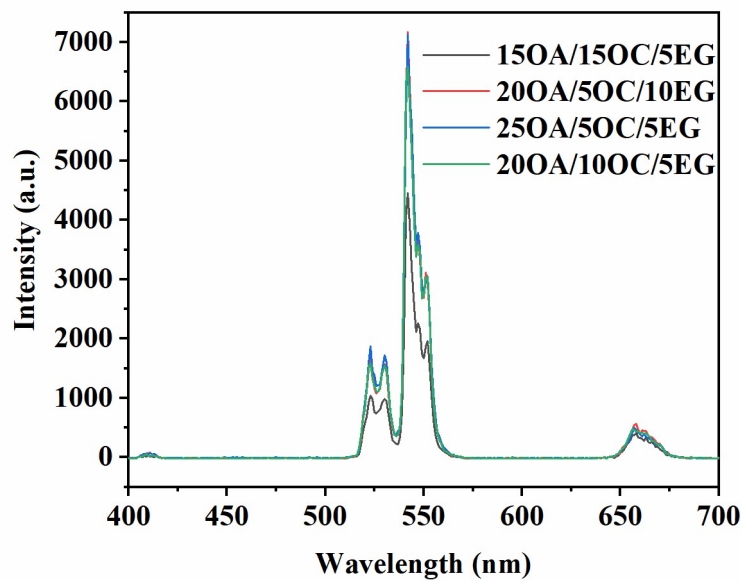
Figure S3. Upconversion emission spectra of $Na_{0.9}Ca_{0.9}Gd_{1.1}F_6$:$Yb^{3+}$/$Er^{3+}$ nanocrystals under the 980 nm laser diode (LD) excitation (1.86 W/cm^2). All samples prepared under different solvent ratios were dispersed in dimethyl sulphoxide (DMSO) solvent (concentration: 1 mg/mL). Other conditions: 8 mmol NaF, 200 °C for 48 h.
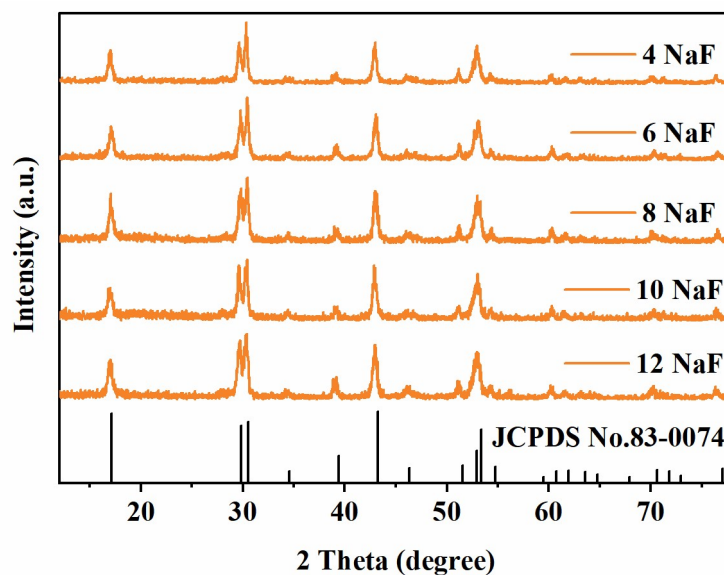

Figure S4. XRD patterns of $Na_{0.9}Ca_{0.9}Gd_{1.1}F_6$:$Yb^{3+}$/$Er^{3+}$ nanocrystals prepared at different NaF concentrations. Other conditions: 200 °C for 48 h, 20 mL OA / 10 mL OC / 5 mL EG.

Table S2. The average size of $Na_{0.9}Ca_{0.9}Gd_{1.1}F_6$:$Yb^{3+}$/$Er^{3+}$ nanocrystals prepared at different NaF concentrations was calculated using the Debye-Scherrer equation. Other conditions: 200 °C for 48 h, 20 mL OA / 10 mL OC / 5 mL EG.

Concentration of NaF (mmol)	sizes (nm)
4.0	24.7
6.0	22.0
8.0	20.9
10.0	22.3
12.0	19.2
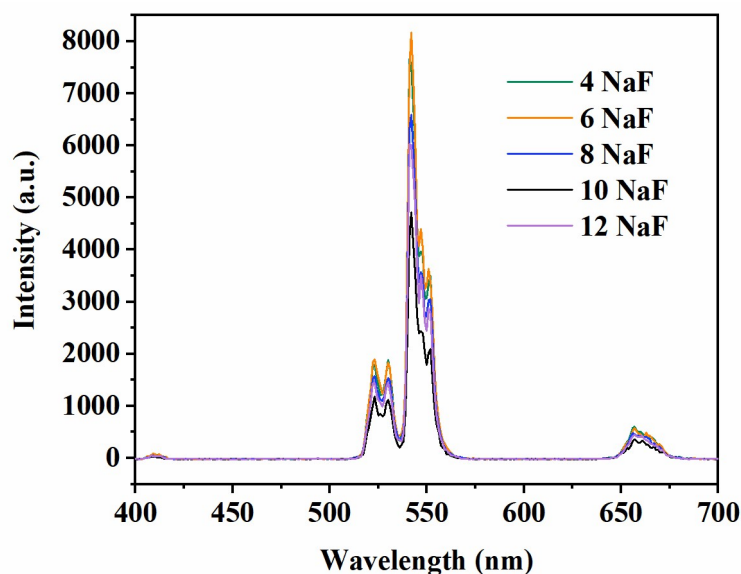
Figure S5. Upconversion emission spectra of $Na_{0.9}Ca_{0.9}Gd_{1.1}F_6$:$Yb^{3+}$/$Er^{3+}$ nanocrystals under the 980 nm laser diode (LD) excitation (1.86 W/cm^2). All samples prepared at different NaF concentrations were dispersed in dimethyl sulphoxide (DMSO) solvent (concentration: 1 mg/mL). Other conditions: 200 °C for 48 h, 20 mL OA / 10 mL OC / 5 mL EG.
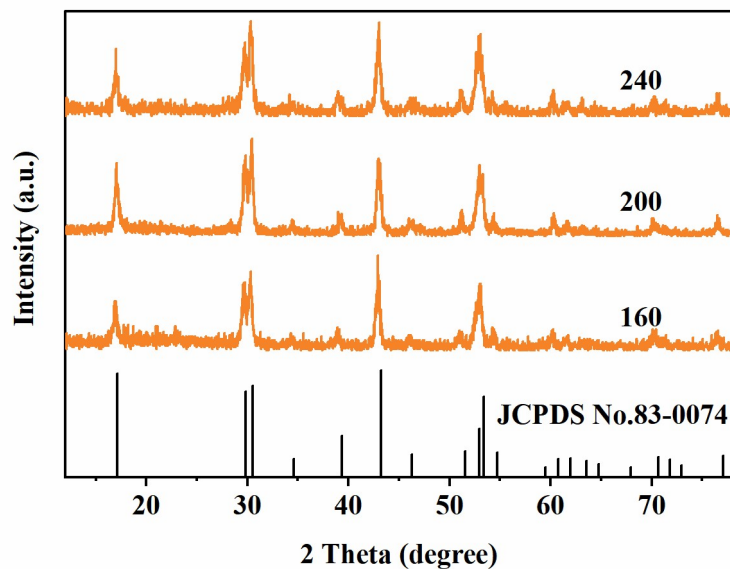
Figure S6. XRD patterns of $Na_{0.9}Ca_{0.9}Gd_{1.1}F_6$:$Yb^{3+}$/$Er^{3+}$ nanocrystals synthesized at different reaction temperatures (°C). Other conditions: 8 mmol NaF, 48 h, 20 mL OA / 10 mL OC / 5 mL EG.

Table S3. The average size of $Na_{0.9}Ca_{0.9}Gd_{1.1}F_6$:$Yb^{3+}$/$Er^{3+}$ nanocrystals prepared at different reaction temperatures was calculated using the Debye-Scherrer equation. Other conditions: 8 mmol NaF, 48 h, 20 mL OA / 10 mL OC / 5 mL EG.

reaction temperature (°C)	sizes (nm)
240 °C	19.4
200 °C	20.9
160 °C	22.5

6
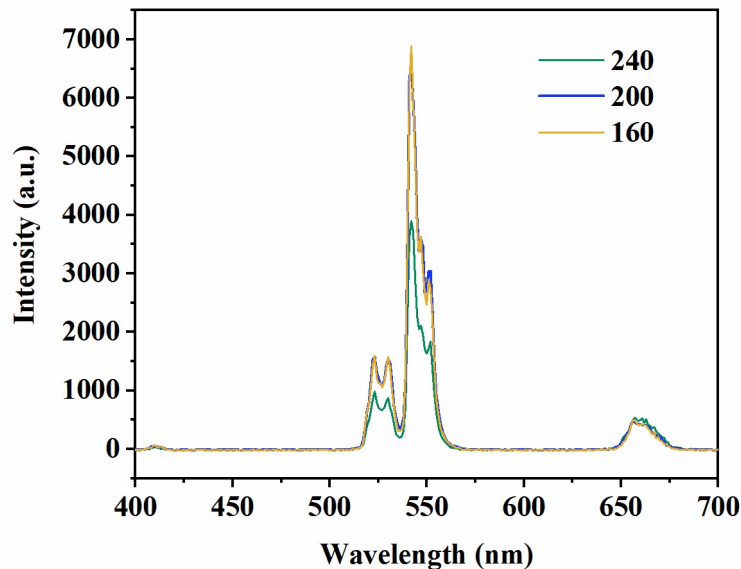
Figure S7. Upconversion emission spectra of $Na_{0.9}Ca_{0.9}Gd_{1.1}F_6$:$Yb^{3+}$/$Er^{3+}$ nanocrystals under the 980 nm laser diode (LD) excitation (1.86 W/cm^2). All samples prepared at different reaction temperatures were dispersed in dimethyl sulphoxide (DMSO) solvent (concentration: 1 mg/mL). Other conditions: 8 mmol NaF, 48 h, 20 mL OA / 10 mL OC / 5 mL EG.
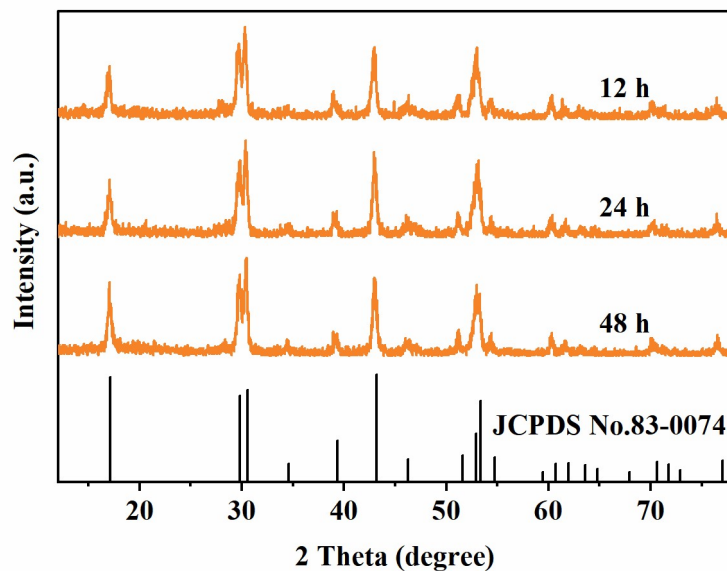

Figure S8. XRD patterns of $Na_{0.9}Ca_{0.9}Gd_{1.1}F_6$:$Yb^{3+}$/$Er^{3+}$ nanocrystals synthesized at different reaction times. Other conditions: 8 mmol NaF, 200 °C, 20 mL OA / 10 mL OC / 5 mL EG.

Table S4. The average size of $Na_{0.9}Ca_{0.9}Gd_{1.1}F_6$:$Yb^{3+}$/$Er^{3+}$ nanocrystals prepared at different reaction times was calculated using the Debye-Scherrer equation. Other conditions: 8 mmol NaF, 200 °C, 20 mL OA / 10 mL OC / 5mL EG.
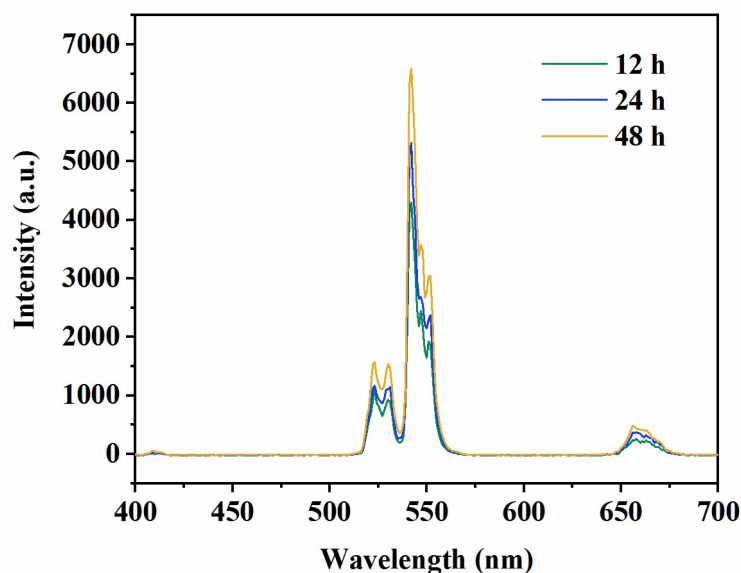
reaction time (hour)	sizes (nm)
12 h	17.6
24 h	18.4
48 h	20.9

Figure S9. Upconversion emission spectra of $Na_{0.9}Ca_{0.9}Gd_{1.1}F_6$:$Yb^{3+}$/$Er^{3+}$ nanocrystals under the 980 nm laser diode (LD) excitation (1.86 W/cm^2). All samples prepared at different eaction times were dispersed in dimethyl sulphoxide (DMSO) solvent (concentration: 1 mg/mL). Other conditions: 8 mmol NaF, 200 °C, 20 mL OA / 10 mL OC / 5mL EG.
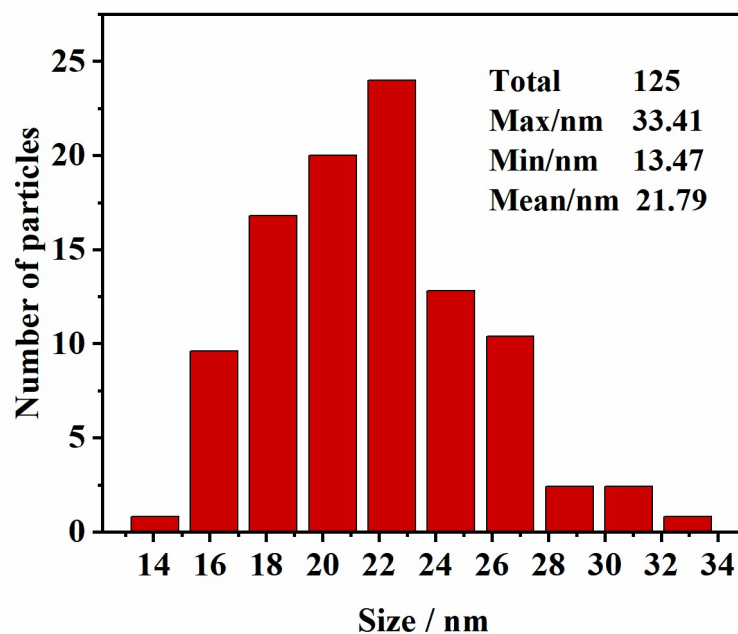
Figure S10. Histogram of the average diameter of $Na_{0.9}Ca_{0.9}Gd_{1.1}F_6$:$Yb^{3+}$/$Er^{3+}$ nanorods synthesized under 8 mmol NaF, 20 mL OA, 10 mL OC, 5 mL EG, at 200 °C for 48 h. (standard deviation (σ): 3.71)

Figure S11. Histogram of the average length of $Na_{0.9}Ca_{0.9}Gd_{1.1}F_6$:$Yb^{3+}$/$Er^{3+}$ nanorods synthesized under 8 mmol NaF, 20 mL OA, 10 mL OC, 5 mL EG, at 200 °C for 48 h. (standard deviation (σ): 6.52)
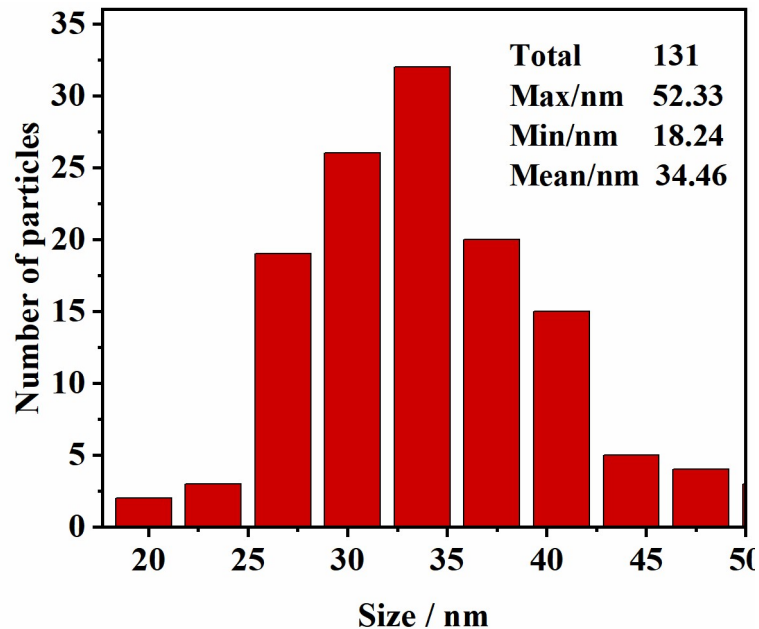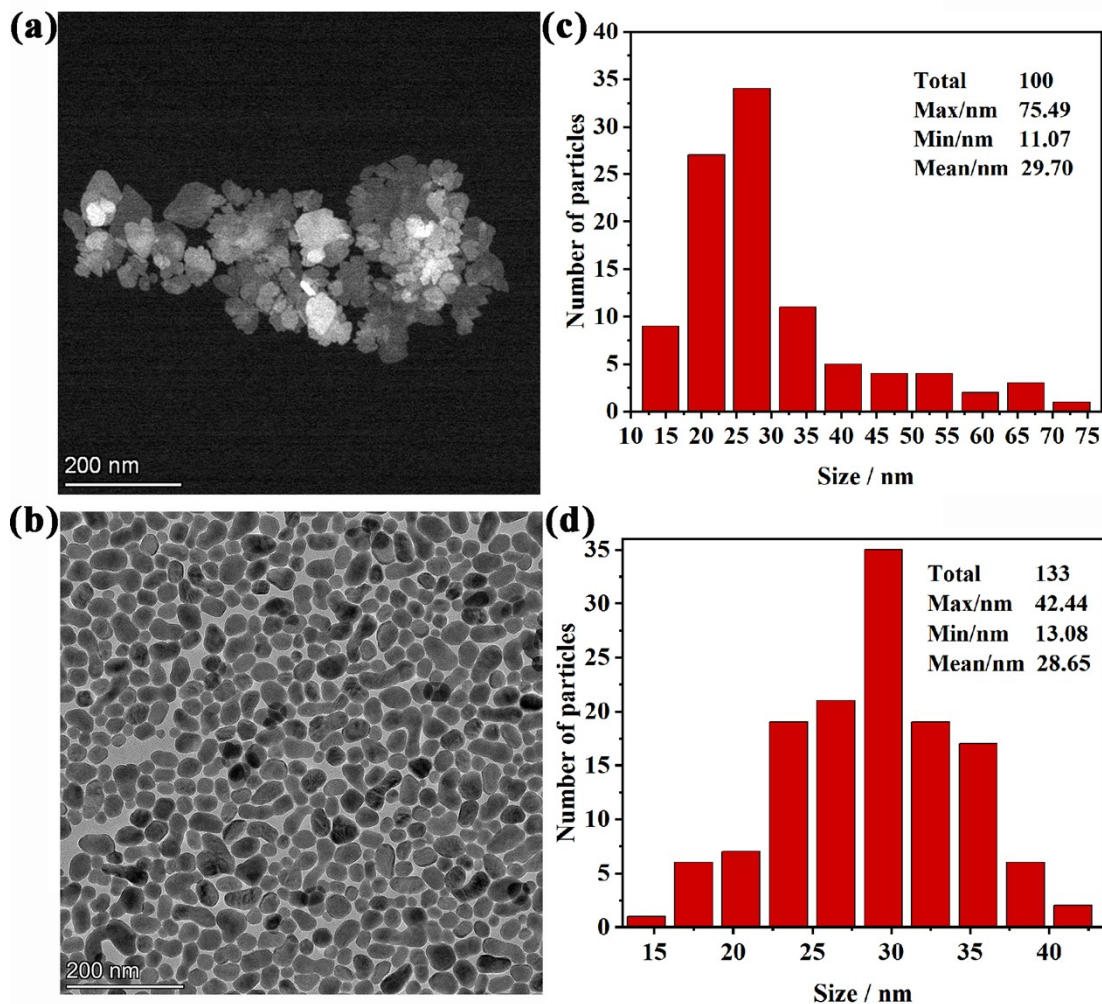
Figure S12. (a) TEM of orthorhombic-phase GdF_3:Yb^{3+}/Er^{3+} NPs synthesized under 1.5 mmol LiF, 20 mL OA, 10 mL OC, 5 mL EG, at 200 °C for 48 h. (b) TEM of hexagonal-phase $NaGdF_4$:Yb^{3+}/Er^{3+} NPs synthesized under 8 mmol NaF, 20 mL OA, 10 mL OC, 5 mL EG, at 200 °C for 48 h. (c) Histogram of the average particle size of orthorhombic-phase GdF_3:Yb^{3+}/Er^{3+} NPs synthesized under 1.5 mmol LiF, 20 mL OA, 10 mL OC, 5 mL EG, at 200 °C for 48 h (standard deviation (σ): 12.60). (d) Histogram of the average particle size of hexagonal-phase $NaGdF_4$:Yb^{3+}/Er^{3+} NPs synthesized under 8 mmol NaF, 20 mL OA, 10 mL OC, 5 mL EG, at 200 °C for 48 h (standard deviation (σ): 5.45).
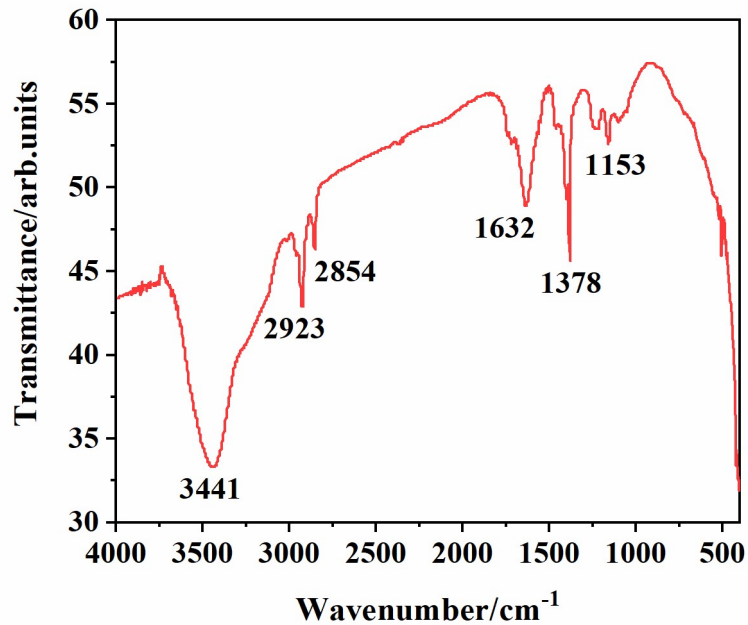
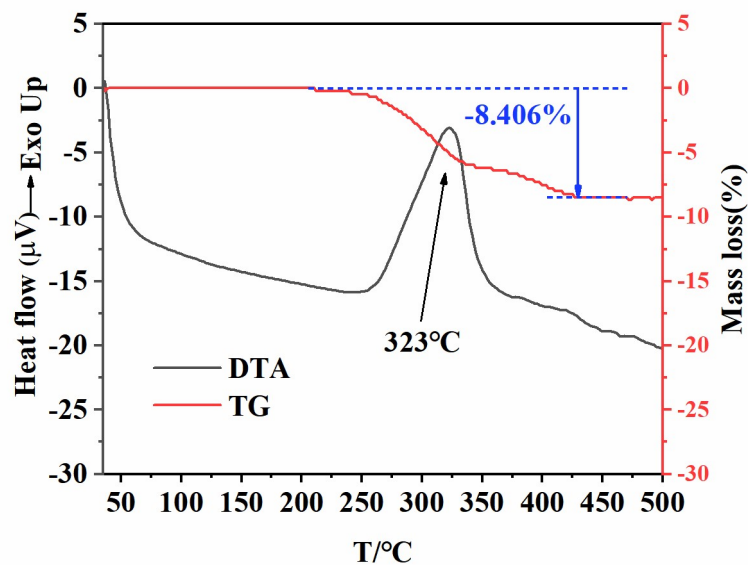**Figure S13.** Fourier transform infrared (FTIR) spectra of the prepared hexagonal Yb^{3+}/Er^{3+} co-doped $Na_{0.9}Ca_{0.9}Gd_{1.1}F_6$ nanorods.

Figure S14. The DTA-TG (differential thermal ananlysis-thermogravimetry) curves of Yb^{3+}/Er^{3+} co-doped $Na_{0.9}Ca_{0.9}Gd_{1.1}F_6$.
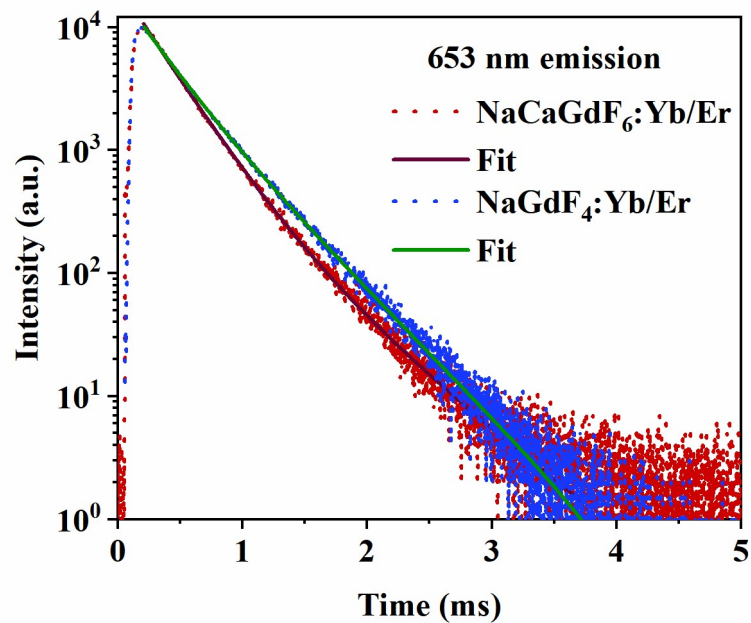
Figure S15. Decay curves of $NaGdF_4$:Yb^{3+}/Er^{3+} (25 nm) and $Na_{0.9}Ca_{0.9}Gd_{1.1}F_6$:$Yb^{3+}$/$Er^{3+}$ (21 nm) nanocrystals at 653 nm (Er^{3+}).
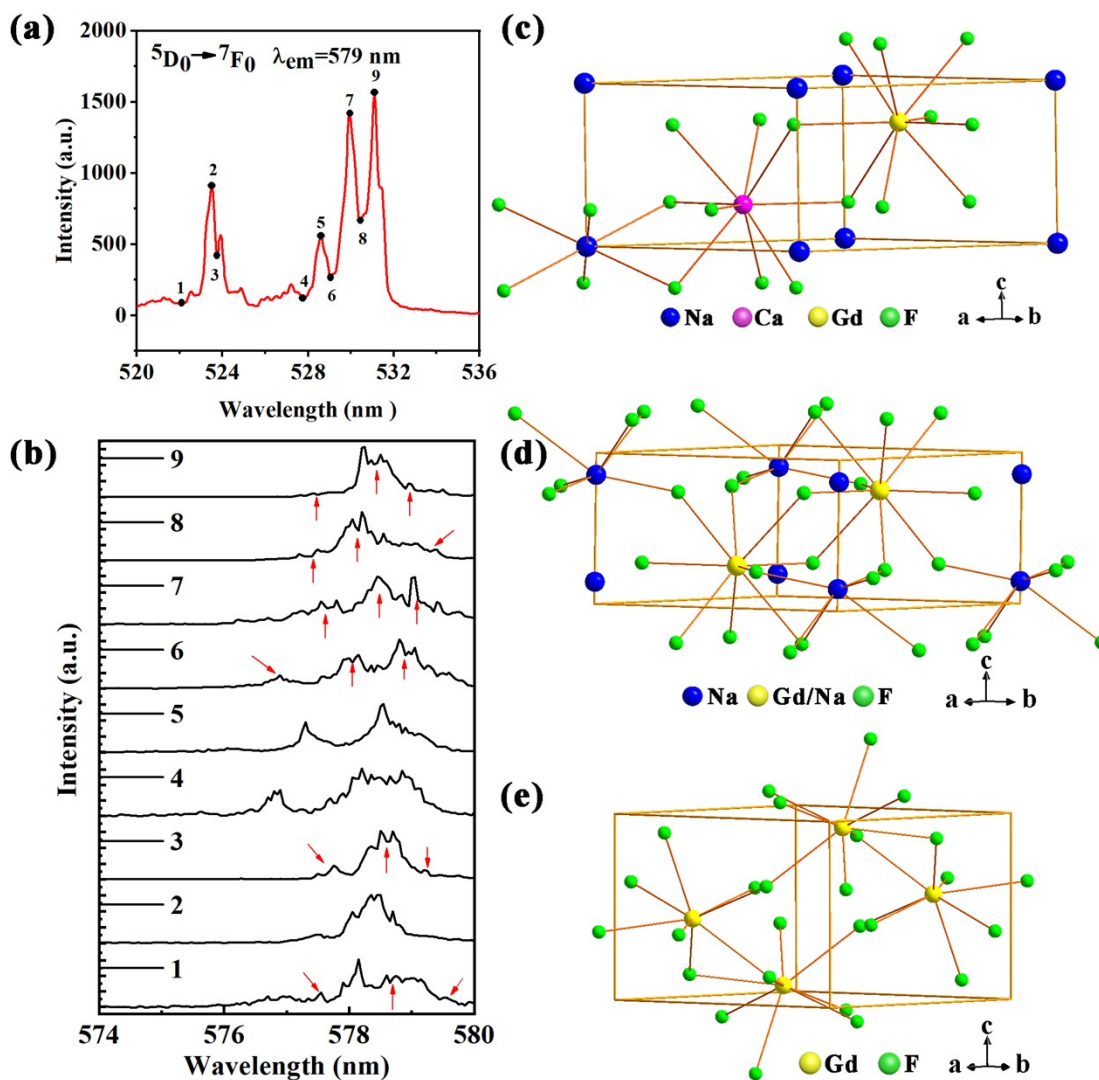
Figure S16. (a) The $^5D_0 \rightarrow {}^7F_0$ excitation spectra of monitoring 579 nm. (b) site-selective emission spectra of $Na_{0.9}Ca_{0.9}Gd_{1.1}F_6$:$Eu^{3+}$ at 11 K. (c) The structure diagram of hexagonal-phase $Na_{0.9}Ca_{0.9}Gd_{1.1}F_6$:Yb/Er.[2] (d) The structure diagram of hexagonal-phase $NaGdF_4$:Yb/Er.[3] (e) The structure diagram of orthorhombic-phase GdF_3:Yb/Er.[4]

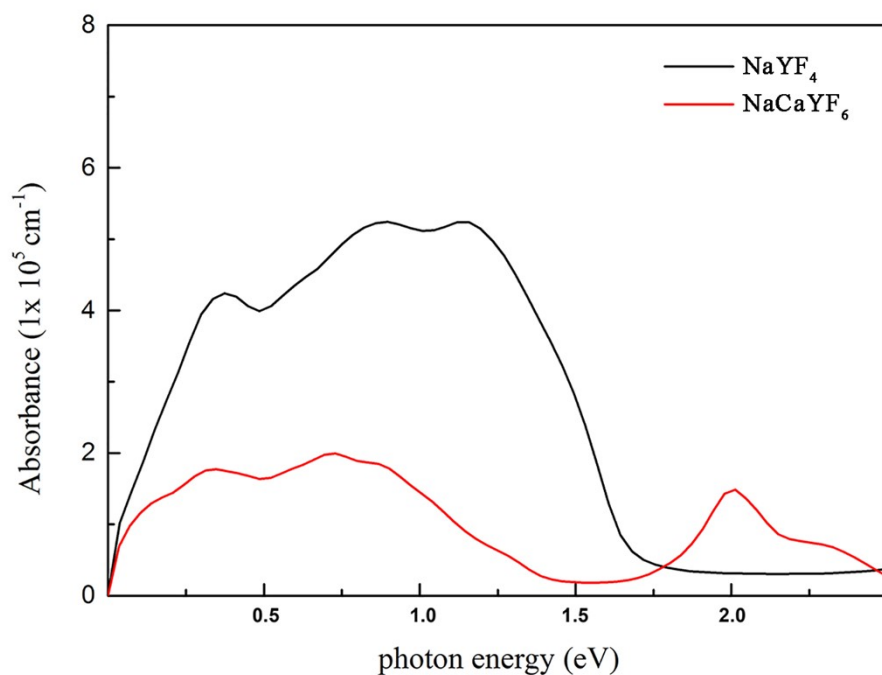**Figure S17.** First-principles calculations of the photon absorption ranges and intensities of $Na_{0.9}Ca_{0.9}Y_{1.1}F_6$ and $NaYF_4$ host materials. (Photon energies less than 1.5 eV were confirmed to be in the infrared region, and the calculation results of $Na_{0.9}Ca_{0.9}Gd_{1.1}F_6$ and $Na_{0.9}Ca_{0.9}Y_{1.1}F_6$ were similar.)
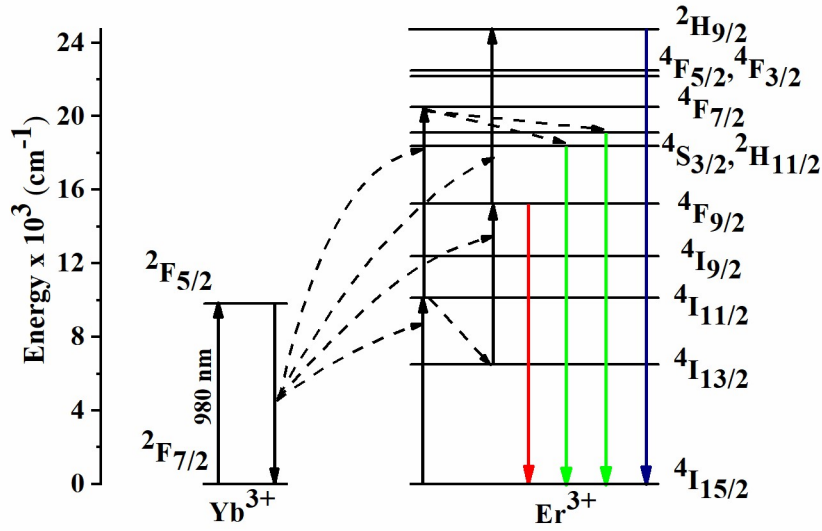
Figure S18. Energy level diagram of the upconversion luminescence of Yb^{3+}/Er^{3+} co-doped GdF_3, $NaGdF_4$, and $Na_{0.9}Ca_{0.9}Gd_{1.1}F_6$ samples under 980 nm laser excitation.

Under 980nm LD excitation, the sensitizer Yb^{3+} ions transition from ground state energy level $^2F_{7/2}$ to excited state energy level $^2F_{5/2}$. Yb^{3+} transfers the energy of nonradiative transition back to ground state to the nearby activator Er^{3+} ions, resulting in the transition of Er^{3+} ions from $^4I_{15/2}$ level to $^4I_{11/2}$ level, and the Er^{3+} ions at $^4I_{11/2}$ level absorb the energy of Yb^{3+} ions again to higher $^4F_{7/2}$ level. The Er^{3+} ions at the $^4F_{7/2}$ level transition to the $^2H_{11/2}$ and $^4S_{3/2}$ levels through non-radiative relaxation. Both processes from the $^2H_{11/2}$ and $^4S_{3/2}$ energy levels to the $^4I_{15/2}$ energy level can produce green emission. Er^{3+} ions at $^4I_{11/2}$ level relax to $^4I_{13/2}$ level by nonradiative relaxation, and then further absorb the energy of Yb^{3+} ions to $^4F_{9/2}$ level. The transition from $^4F_{9/2}$ level to $^4I_{15/2}$ level produces red emission. In addition, the Er^{3+} ions at the $^4F_{9/2}$ energy level can absorb the energy from the Yb^{3+} ions and transition to the $^2H_{9/2}$ energy level, and the transition from the $^2H_{9/2}$ energy level to the $^4I_{15/2}$ energy level produces blue emission.

References

1 Y. Xu, Z. Zeng, D. Zhang, S. Liu, X. Wang, S. Li, C. Cheng, J. Wang, Y. Liu, G. De, C. Zhang, W. Qin and Y. Du, *Adv. Opt. Mater.*, 2020, **8**, 1901495.

2 J. M. Hughes and J. W. Drexler, *Can. Mineral.*, 1994, **32**, 563-565.

3 F. Wang, Y. Han, C. S. Lim, Y. Lu, J. Wang, J. Xu, H. Chen, C. Zhang, M. Hong and X. Liu, *Nature*, 2010, **463**, 1061-1065.

4 Y. Tian, H.-Y. Yang, K. Li and X. Jin, *J. Mater. Chem.*, 2012, **22**, 22510-22516.